Lawrence Berkeley National Laboratory

Title
Synthesis, Structure, and Ionic Conductivity of Self-Assembled Amphiphilic Poly(methacrylate) Comb Polymers

Authors
Liu, Gao
Reinhout, Melanie
Mainguy, Brian
et al.

Synthesis, Structure, and Ionic Conductivity of Self-Assembled Amphiphilic Poly(methacrylate) Comb Polymers

Gao Liu,^ Melanie Reinhout, Brian Mainguy, and Gregory L. Baker*

Department of Chemistry, Michigan State University, East Lansing, Michigan 4882.

phone: (517) 355-9715 ext. 160, bakerg@msu.edu

TITLE RUNNING HEAD Self-Assembled Amphiphilic Poly(methacrylic) Combs

^ Present address: Lawrence Berkeley National Laboratory, 1 Cyclotron Rd., MS 70R108B, Berkeley, CA 94720

ABSTRACT

Methacrylate comb polymers were synthesized that have amphiphilic teeth of ethylene glycol oligomers capped with alkyl groups. Both segments are of exact length to promote self-organization and crystallization. The atactic methacrylate backbone plus close proximity to the polymer backbone inhibits crystallization of the oligoethyelene oxide segments, but the terminal alkyl segments readily crystallize. Wide angle x-ray diffraction and differential scanning calorimetry were used to characterize polymer side chain crystallization and its evolution as a function of the length of the amphiphilic teeth. An analysis of the d-spacings places the oligoethylene glycol segment and the first 8 carbon atoms of the alkyl chain in an amorphous phase. An ~1Å/carbon atom increase in the d-spacing is consistent with the crystalline segments being tilted relative to the polymer backbone. When the number of carbon atoms in alkyl segments is ≥ 14, addition of $LiClO_4$ yields an ionic conducting ethylene oxide phase with retention of the alkyl crystallization. These novel polymer electrolytes use crystallization as a structural element to maintain dimensional stability.

KEYWORDS Keywords: comb polymer, polymer electrolyte, nanostructure, self-assembly.

INTRODUCTION

Polymeric materials capable of transporting small molecules and ions find important applications in membrane-based separations,[1-3] and as electrolytes for sensors, fuel cells[4-8] and lithium batteries.[9-11] An ongoing challenge in the design of polymer electrolytes is to combine the high ionic conductivity of liquid electrolytes with the mechanical properties typical of thermoplastics in a single material.[12] Ion transport in polymers is usually related to the polymer free volume and segmental motion, and thus ions and neutral molecules diffuse more rapidly through polymers at temperatures above their glass transition (T_g). However, the use of polymers at $T>T_g$ has serious drawbacks since most polymers have poor dimensional stability above T_g. Well known strategies for stabilizing polymers such as crosslinking[13] effectively render polymer electrolytes dimensionally stable. However, most cross-linking strategies also reduce chain mobility, and since ionic mobility in polyether electrolytes is tied to the flexibility of the polymer chain, the corresponding conductivity also declines. The most successful solutions to this problem have been multiphase materials such as gels,[14] block copolymers,[15, 16] and nanoparticulate composites[17-20] that simplify the electrolyte design process by decoupling the structural elements that correlate to high conductivity from those that lead to good mechanical properties. A common feature in these systems is a continuous reinforcing phase that provides dimensional stability to a low molecular weight liquid electrolyte.

One design element that is largely overlooked is the use of polymer crystallization to enhance dimensional stability. Crystallinity has long been viewed as being detrimental to achieving high conductivity in polymer electrolytes since the fixed position of atoms in a crystal lattice is incompatible with most ion conduction mechanisms. However, as long as crystallinity is restricted to the insulating portion of the polymer, it should be possible to design a two-phase system where crystallization of the non-conducting phase has a minimal effect on ion transport in a second phase. Polymers that self-assemble into two-phases, one rubbery and conducive to ion transport, and a rigid crystalline phase that provides dimensional stability, are attractive architectures for testing this strategy.

Polymer combs with oligoethylene oxide teeth are good ionic conductors because of the high flexibility of short oligoethylene oxide chains.[21-34] Since the T_gs of methacrylate-based combs decrease as the length of the oligoethylene oxide side chain increases,[35] most are not dimensionally stable and they typically need to be cross-linked. In general, the glass transition cannot be relied upon to provide mechanical stability in single phase electrolytes, and even poly(*p*-phenylene)s soften and flow when the PEO side chains are long enough to screen the interactions between rigid rod backbones.[36] An alternative to cross-linking is to mimic the morphology of thermoplastic elastomers and use phase separation to form a high T_g or crystalline phase.[12] This can be accomplished by attaching a hydrophobic block to one or both ends of the comb polymer backbone. A second approach, which we explore in this report, is to attach short alkyl chains to the end of the oligoethylene oxide teeth to render them amphiphilic. In the resulting structure, we expect the ethylene oxide portion of the comb will facilitate ion transport while the alkyl tails will crystallize and provide dimensional stability.

Comb-like polymer systems containing long alkyl groups have been extensively investigated[37, 38] and include poly(*n*-alkyl acrylates),[38-41] poly(*n*-alkyl methacrylates),[39, 42] poly(acrylamides),[38, 43] poly(α-olefins),[44, 45] aromatic polyesters,[46] polyamides,[47] polythiophenes[48] and other polymers. Comb systems typically assemble into an overall lamellar structure with the side chains interdigitated or packed end-to-end to form a separate crystalline domain.[37, 49] Differential Scanning Calorimetry (DSC), wide-angle x-ray scattering (WAXS), small-angle x-ray scattering (SAXS), polarized optical microscopy and other techniques show that regardless of the rigidity and tacticity of the backbone, the side-chains of linear alkyl comb polymers crystallize in a hexagonal crystal structure when the length of the side chain exceeds a critical number of methylene groups, usually 7-10.[37, 38, 49] Only the terminal part of the alkyl chains takes part in the crystallization process; the first few atoms attached to the polymer backbone are usually amorphous. For a homologous series of comb polymers, the melting points of the polymers increase with the length of the side chain.
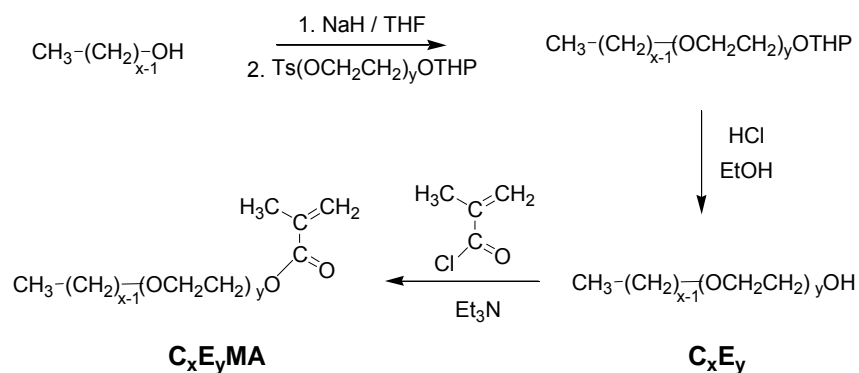
In this report we describe the synthesis and characterization of several series of methacrylate-based combs whose teeth are oligoethylene oxide monoalkyl ethers. In our polymer design, we

sandwich amorphous, ion conducting PEO layers between two insulating layers of crystalline alkyl groups. Alkyl groups placed at the terminus of the teeth favor intermolecular crystallization of the combs and dimensional stability. Adding $LiClO_4$ converts the combs to ionic conductors which have good conductivity, but with retention of the alkyl segment crystallinity.

RESULTS

Since one of our goals is to understand the self-assembly process in amphiphilic comb polymers, we designed comb structures where each tooth is identical in composition and length. We anticipated that eliminating dispersion in the length of the teeth should simplify structural analysis and favor crystallization of the alkyl portion of the side chain. As shown in *Scheme I*, the desired methacrylate monomers are readily available from the reaction of methacryloyl chloride with exact length oligoethylene glycol monoalkyl ethers, which in turn can be obtained in high yield and purity via an iterative process used to prepare exact length oligoethylene glycol dialkyl ethers.[50] The key step in the chain extension process is the use of monotosylated glycols. These crystalline intermediates can be prepared and purified on large scales, enabling us to prepare monodisperse ethylene glycols with degrees of polymerization as high as 14. The methacrylate monomers were purified by column chromatography and polymerized at 60 °C using AIBN as the initiator. After isolation by precipitation into methanol, the polymers were dried under vacuum. At room temperature, polymers with short side chains are best

Scheme 1

$$CH_3-(CH_2)_{x-1}-OH \xrightarrow[\text{2. Ts(OCH}_2CH_2)_yOTHP]{\text{1. NaH / THF}} CH_3-(CH_2)_{x-1}(OCH_2CH_2)_yOTHP$$

$$\downarrow \begin{array}{c} HCl \\ EtOH \end{array}$$

$$CH_3-(CH_2)_{x-1}(OCH_2CH_2)_yO \xleftarrow[\text{Et}_3N]{} CH_3-(CH_2)_{x-1}(OCH_2CH_2)_yOH$$

$$\mathbf{C_xE_yMA} \qquad\qquad \mathbf{C_xE_y}$$

described as translucent gels, while those with longer side chains are white crystalline powders. For convenience, these methacrylate polymers are abbreviated as poly(C_xE_yMA), where x and y refer to the number of structural repeat units in the alkyl and oligoethylene oxide segments, respectively, while MA identifies the methacrylate backbone of the polymer.

The molecular characterization data for these polymers are shown in ***Table 1***. In all cases, the polymers have high molecular weights and polydispersities typical of free-radical polymerizations. We considered using ATRP to obtain polymers with narrower molecular weight distributions, but our experience to date with the ATRP of PEG methacrylates suggests that it would be difficult to completely remove the metal catalyst from the polymer, which may introduce some uncertainty in interpreting the conductivity data.

Table 1. Physical properties of amphiphilic methacrylate polymers (poly(C_xE_yMA))

polymer	M_w ($\times 10^{-3}$)	PDI	T_g (°C)[a]	mp (°C)	ΔH_{fus} (J/g)	d spacing (Å)
poly(C_6E_0MA)	116	2.2	-21	-	-	
poly(C_6E_2MA)	43.3	2.3	-71	-	-	
poly(C_6E_4MA)	207	2.0	-68	-	-	
poly(C_6E_6MA)	69.8	1.5	*nd*	-	-	
poly(C_8E_4MA)	123	2.5	-66	-	-	
poly($C_{10}E_4MA$)	107	3.0	-63	-	-	
poly($C_{12}E_4MA$)	306	2.0	-65	-1.8	28	37.7[b]
poly($C_{14}E_0MA$)	100	2.5	-22	-7.0	18	28.1[b]
poly($C_{14}E_2MA$)	153	2.9	*nd*	18.0	37	32.7[b]
poly($C_{14}E_4MA$)	171	3.1	-39	21.9	43	37.4[b]
poly($C_{14}E_6MA$)	69.0	1.6	*nd*	16.6	38	46.3[b]
poly($C_{16}E_4MA$)	173	3.3	*nd*	37.3	52	41.4
poly($C_{18}E_4MA$)	183	2.9	-20	48.9	60	43.1

a. Samples where no glass transitions were detected are labeled *nd*

**b**. measured at -50 °C

The thermal properties of the polymers were measured by DSC under helium at a heating rate of 10°/min. All samples were initially heated to above their melting points to erase any thermal history induced by the workup procedure or long-term storage of the polymers. The data shown in ***Figures 1*** and ***2*** are second heating scans taken after quenching the samples from the melt. For the E = 4 series of
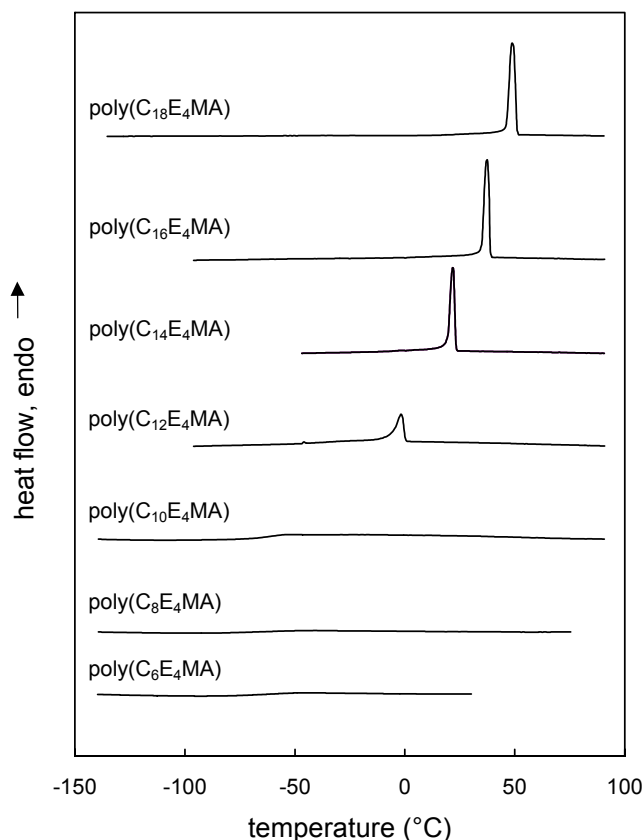

Figure 1. DSC data showing the melting behavior of amphiphilic C_xE_4 poly(methacrylate) combs. Shown are second heating scans measured under He at 10 °/min taken after erasing the thermal history of the sample at 60°.

polymers (Figure 3, triangles), a dodecyl chain was the minimum alkyl chain length that led to observable crystallinity. Glass transitions were seen for polymers with branches shorter than C_{12}, but no evidence of crystallization. The melting points for the polymers (***Table 1***) steadily increase with increases in the length of the alkyl segment, reaching 49 °C for a C_{18} segment. This behavior mirrors
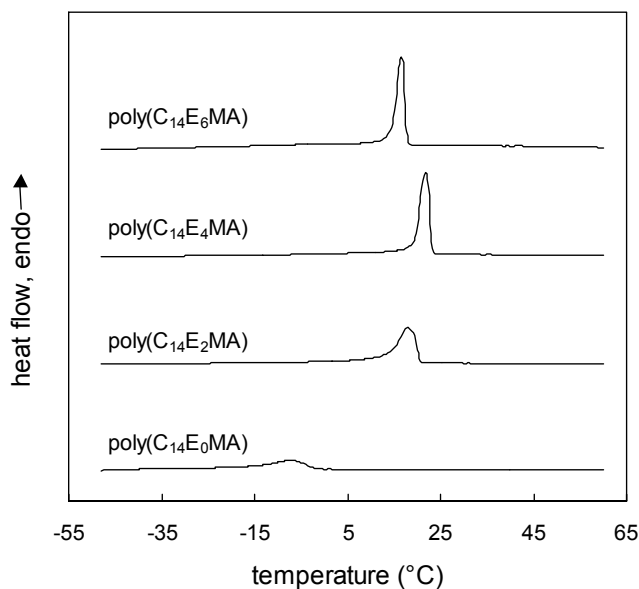
Figure 2. DSC data showing the melting behavior of amphiphilic $C_{14}E_y$ poly(methacrylate) combs. Shown are second heating scans measured under He at 10 °/min taken after erasing the thermal history of the sample at 60°.

that of poly(*n*-alkyl methacrylates), where crystallization is first observed for poly(dodecyl methacrylate) (mp = -34 °C),[39] and the melting point for poly(octadecyl methacylate)s is 34 °C.[39] In like manner, the ΔH_{fus} values increased from 23 J/g for C=12 to 60 J/g for C=18 indicating a steady growth in crystallinity as more methylenes are included in the crystalline domains.
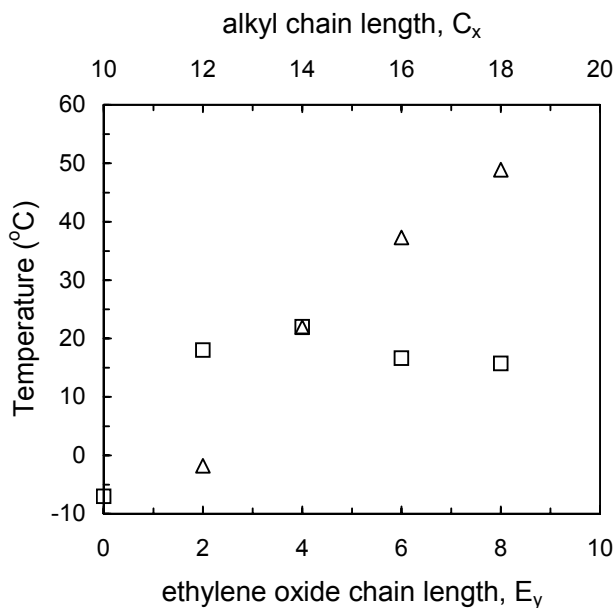

Figure 3. Dependence of the polymer melting point on the length of the alkyl and ethylene oxide segments in amphiphilic poly(methacrylate) combs; triangles: C_xE_4 series, squares $C_{14}E_y$ series.

7

In contrast, the addition of ethylene oxide segments to the amphiphilic side chains makes only minor contributions to polymer crystallinity. Shown in *Figure 2* are DSC data for a series of $C_{14}E_y$ polymers. Using poly(tetradecyl methacrylate) (polyC$_{14}$E$_0$) as a reference, introducing two ethylene oxide segments increases the melting point from -7 °C to 18°, but both the melting points and ΔH_{fus} values are nearly constant as the ethylene oxide segment is lengthened further. The trends in the melting points for these two sets of polymers are more clearly seen in *Figure 3*.

A plausible rationale for the data is that the crystallinity in these polymers is due solely to the C_{14} chain, and the ethylene oxide segments, being bound directly to the polymer backbone, simply act as amorphous spacers and do not enter into the crystalline regions. Confirmation comes from an analysis of ΔH_{fus} as a function of the number of chain atoms in the teeth of the combs. Studies of a number of comb polymers having *n*-alkyl teeth show that for limited ranges of n, ΔH_{fus} is linearly dependent on n
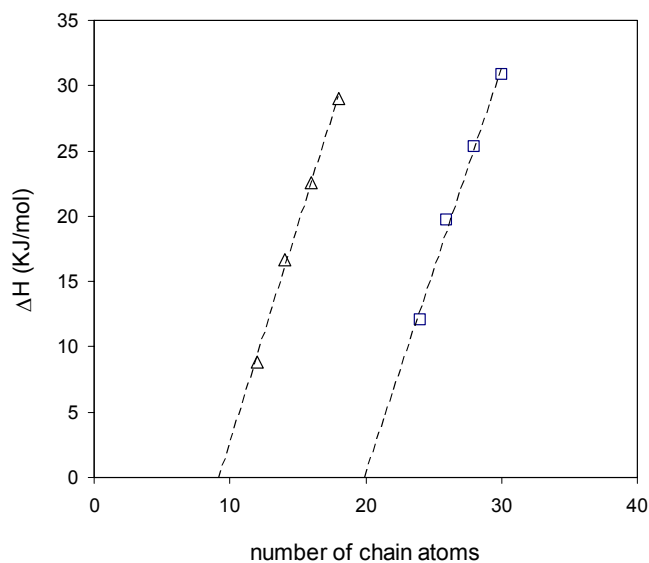

Figure 4. Dependence of ΔH_{fus} on the number of chain atoms in the teeth of poly(*n*-alkyl acrylate)s[38] (triangles) and amphiphilic poly(C$_x$E$_4$MA) combs (squares).

with a slope of ~3.3 KJ/mol CH$_2$ with the x-intercepts interpreted as the number of amorphous chain atoms in the teeth.[38] Plotted in *Figure 4* are data from the poly(C$_x$E$_4$MA) series as well as data from a series of poly(*n*-alkyl methacrylates) reported by Jordan.[38] Both data sets are linear and have similar slopes, but the data from the C$_x$E$_4$MA polymers are shifted to larger numbers of chain atoms. The

intercept for the poly(C_xE_4MA) series corresponds to the 12 atoms of the ethylene oxide segment plus 8 carbon atoms in the alkyl chain compared to ~9 carbon atoms for the poly(*n*-alkyl methacrylate)s, consistent with the data of ***Figure 3*** and with the conclusion that the ethylene oxide units do not participate in crystallization

A key aspect in the design of these polymers was the notion that linking the PEO segments to an atactic methacrylate backbone would suppress the tendency for PEO to crystallize and ensure that the PEO phase remains amorphous to support ionic conductivity. However, there are obvious limits to this approach since these effects should disappear for long PEO segments and for PEO segments placed at the end of the teeth. We note that PEO segments in comparably sized $C_xE_yC_x$ oligomers, not restricted by the atactic backbone, readily crystallize in both planar zig-zag and helical conformations.[50, 51] We do observe a narrowing of the melting transition for longer ethylene oxide segments that implies more ordered crystalline regions when the ethylene oxide spacer is longer.
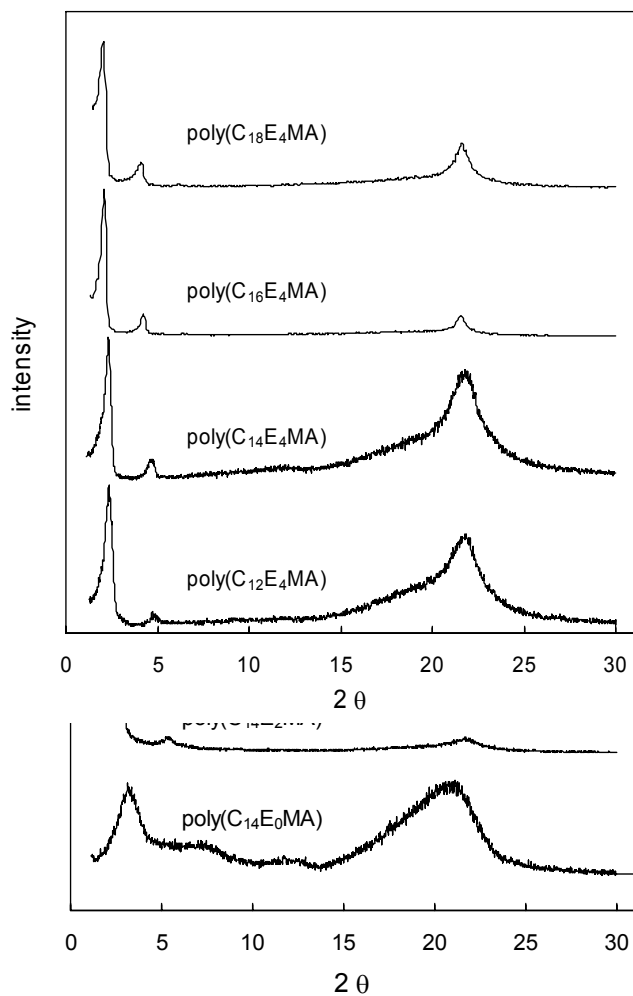
Figure 5. Powder x-ray diffraction data for poly(C_xE_4MA) combs.

Powder pattern x-ray diffraction experiments (***Figures 5*** and ***6***) yield two types of reflections, a wide angle reflection near 21.6°,

9

and reflections at lower angles that are consistent with a layered structure for the crystalline polymers.[37, 49] The reflection at 22.5° (~4.56 Å) is typically observed in comb polymers with long *n*-alkyl teeth and corresponds to hexagonal packing of the alkyl chains.[37, 49] In

Figure 6. Powder x-ray diffraction data for poly($C_{14}E_yMA$) combs.

this case the alkyl chains are somewhat disordered and thus the spacing is slightly higher than the 4.17 Å seen for crystalline normal parafins. The diffraction patterns in the low angle region show a prominent reflection at <5°, as well as second order reflections that are consistent with d-spacings of 28 – 46 Å. As expected, the polymers with the longest side chains had the highest d-spacings. The lowest angle reflection sharpens as the length of the side chain increases, an effect that is more pronounced for the $C_{14}E_y$ series (***Figure 6***). As with the DSC data described earlier, narrowing of the reflection with increases in the length of the E_y segment is consistent with a diminishing effect of the polymer backbone on crystallization, thus leading to a more ordered crystalline phase.

When the d-spacings extracted from the low angle data of *Figures 5* and *6* are plotted as a function of the number of atoms in the side chain of the polymer comb (*Figure 7*), the d-spacings are linearly related to chain length with a slope of ~1 Å/atom. A large number of polymers having *n*-alkyl-substituents have been prepared and analyzed, and a common packing motif for acrylate and methacrylate polymers is a layered structure where the alkyl chains extend from both sides of the polymer backbone.[37, 49] The side chains can pack end to end or they interdigitate. The 1 Å/atom increment is smaller than the 1.24 Å/atom expected for extended interdigitated alkyl chains oriented perpendicular to the polymer backbone. Tilting the chains by ~35° (i.e. a herringbone motif) would be
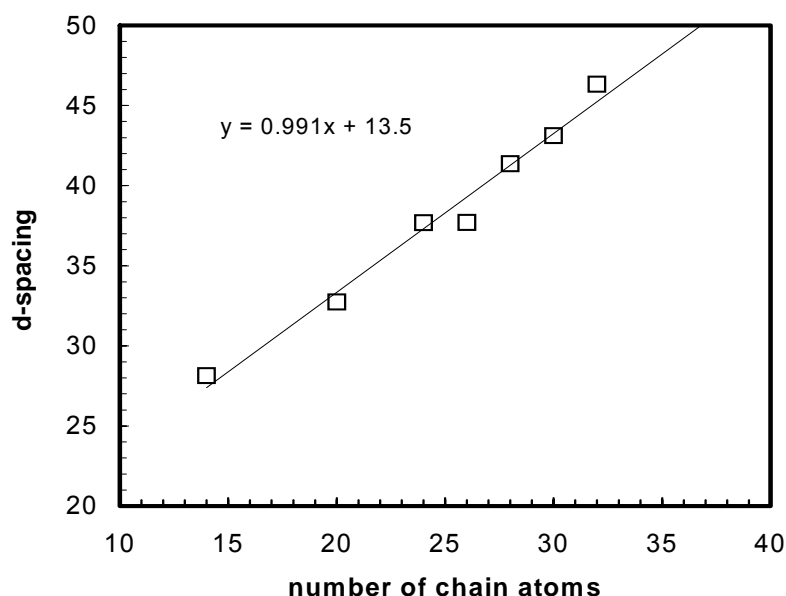

Figure 7. The relationship between the average d-spacing extracted from the x-ray data and the number of chain atoms in the methacrylate side chain. The data are derived from the poly($C_{14}E_yMA$) and poly(C_xE_4MA) series shown in Figures 2 and 4.

consistent with the observed change in spacing, but more extensive x-ray diffraction experiments are needed to define clearly the tilt angle.

Amphiphilic Combs as Polymer Electrolytes. $LiClO_4$ was dissolved in the amphiphilic comb polymers to yield polymer electrolytes. The critical structural issue relevant to our two-phase hypothesis for electrolytes was whether the crystallinity due to the alkyl segments (reinforcing element) would survive the disorder induced by dissolution of the salt to form an ion-conducting phase. The DSC data shown in *Figure 8* for poly($C_{18}E_4MA$) and *Figure 9* for poly($C_{16}E_4MA$) show that crystallinity was preserved in both systems, and that the degree of crystallinity was nearly constant up to

the highest Li$^+$ concentrations. Thus the structure of the electrolytes at room temperature can be viewed as an amorphous polyethyer rendered dimensionally stable by the formation of crystalline domains.

Figure 8. DSC data for electrolytes prepared from LiClO$_4$ and amphiphilic poly(C$_{18}$E$_4$MA) combs. Shown are second heating scans measured under He at 10 °/min, taken after erasing the thermal history of the sample at 60°.
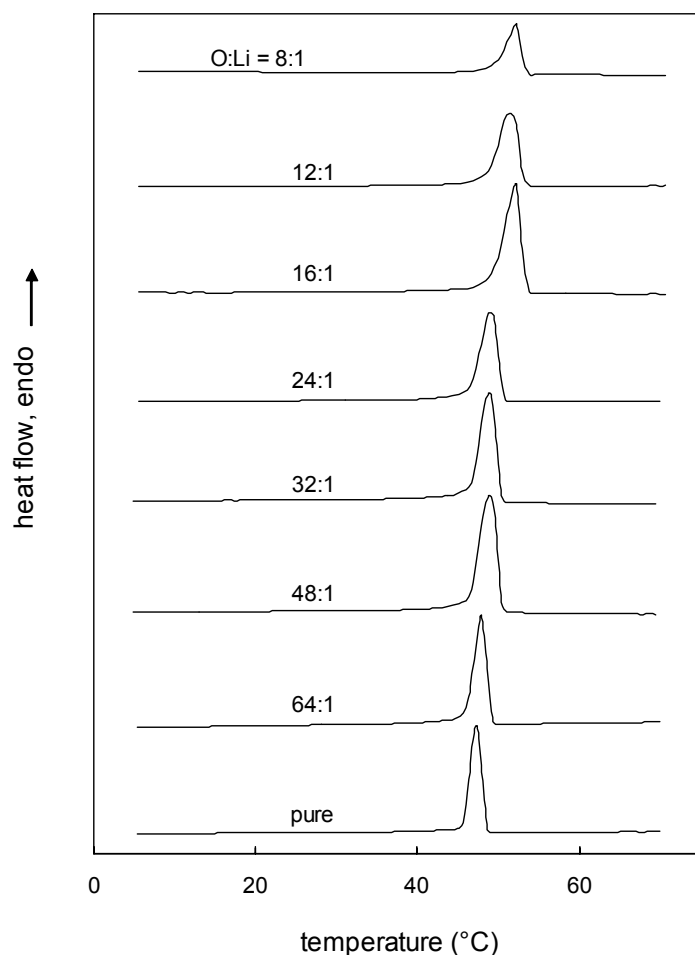
Salt/polymer composites of poly(C$_{16}$E$_4$MA) were characterized by impedance spectroscopy. Because of the relatively low melting points of the polymers, that data in ***Figure 10*** correspond to amorphous, but presumably phase separated samples. The data show that the temperature dependent
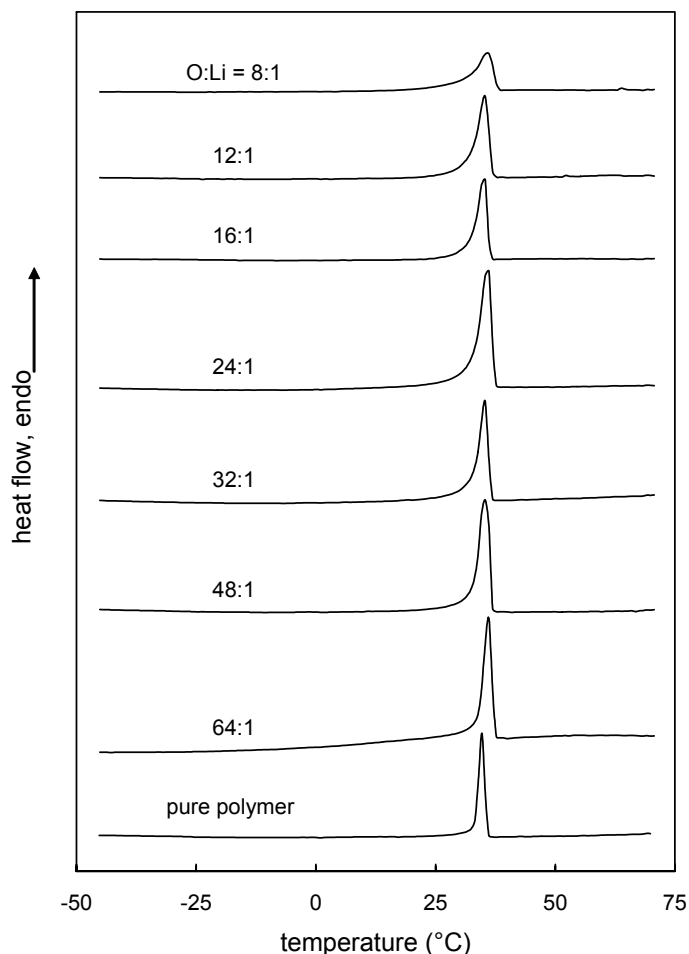
Figure 9. DSC data for electrolytes prepared from $LiClO_4$ and amphiphilic poly($C_{16}E_4MA$) combs. Shown are second heating scans measured under He at 10 °/min, taken after erasing the thermal history of the sample at 60°.

conductivity is sensitive to the level of $LiClO_4$ in the electrolyte, increasing with decreases in the O:Li ratio, and reaching a conductivity maximum at O:Li = 12. For all electrolytes tested, the extrapolated room temperature conductivities were modest, ~10^{-6} S/cm, which is likely related to the low volume fraction of the conducting phase and in the absence of long-range alignment of the ethylene oxide layers, the 2- dimensional nature of the conduction mechanism. The data also revealed some surprising characteristics. We noted that the slope of the log σ vs 1/T plots substantially differ and we were unable to linearize the data by plotting the data vs $1/(T-T_o)$ (VTF plot). While the reason for this behavior is unclear, we speculate that ion concentration strongly influences the microphase separation of the alkyl and ethylene oxide segments in the melt.
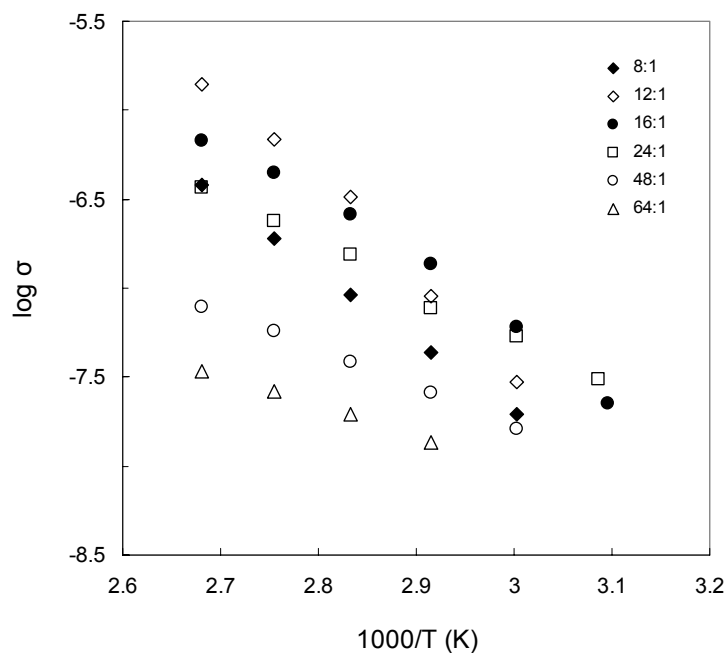
Figure 10. Conductivity of electrolytes prepared from poly($C_{18}E_4MA$) and $LiClO_4$ at various O:Li ratios.

CONCLUSIONS

A series of exact length amphiphilic comb polymethacrylates were synthesized and characterized. These oligoethylene oxide alkyl segments of these polymers micro phase separate to form highly crystalline domains that provide dimensional stability, and amorphous oligoethylene oxide domains that support ionic conductivity. Lithium salts were dissolved into the polymers with retention of the alkyl phase crystallinity. At ambient temperatures these solid polymer electrolytes are crystalline with modest conductivities of $10^{-6} - 10^{-7}$ S/cm.

EXPERIMENTAL SECTION

Unless otherwise noted, all reagents were obtained from Aldrich and were used as received. THF was dried by distillation from sodium benzophenone ketyl. ^{1}H NMR spectra were measured at room temperature in $CDCl_3$ using a Varian Gemini-300 spectrometer at 300 MHz. Chemical shifts were calibrated using residual $CDCl_3$ and are reported in ppm (δ) relative to tetramethylsilane. Differential scanning calorimetry (DSC) measurements were run under helium at a heating rate of 10 ºC/min using a Perkin Elmer DSC 7 calibrated with indium. The reported DSC curves are second heating scans taken after an initial heating scan to erase the thermal history, and a fast quench to −100 °C. X-ray powder diffraction patterns were obtained using a computer controlled Rigaku 200B rotating anode diffractometer operating in reflective mode at 45 kV/100 mA, with graphite monochromatized Cu (K_α) radiation.

All manipulations of the polymers and electrolytes were carried out in a helium drybox. AC impedance data were obtained from an HP 4192A LF Impedance Analyzer scanning from 5Hz to 13MHz with an applied voltage of 10 mV. Data were taken at 30, 40, 50, 60, 70 and 80 °C, with the samples equilibrated at each temperature for at least twenty minutes prior to measurement. The sample cell was constructed of stainless steel disks separated by a Teflon collar. The final dimensions of the sample film have a depth of 0.053 cm and an area of 1.27 cm^2. All electrolytes were prepared in a helium filled dry box by mixing acetonitrile solutions of $LiClO_4$ and the desired polymer. The samples were then concentrated under reduced pressure to afford a viscous solution which was directly cast into the sample holder used for impedance analysis. All composites had an O:Li ratio of 20. Only the oxygen atoms of the polyether chain were included in calculating the O:Li ratio; the carbonyl oxygen was not counted.

2-[2-(2-(2-(2-Tetradecyloxyethoxy)ethoxy)ethoxy)ethoxy]-tetrahydropyran

[$CH_3(CH_2)_{13}(OCH_2CH_2)_4OTHP$]. Under nitrogen, 1-tetradecanol (4.3 g, 20 mmol) was added dropwise to a refluxing suspension of 0.60 g (25 mmol) of sodium hydride in 100 mL of dried THF. After stirring for 30 minutes, a solution of 8.6 g (20 mmol) of the THP-protected tetraethylene glycol

monotosylate in 30 mL THF was added dropwise over a period of 15 min. The mixture was refluxed overnight, cooled to room temperature, and washed with 5% aqueous NaCl (3 × 30 mL). The organic layer was dried over $MgSO_4$ and concentrated under reduced pressure to give a light yellow oil (9.1 g, 96%) which was used without further purification. ^{1}H NMR δ 0.85 (t, 3H), 1.26 (m, 22H), 1.61-1.93 (m, 8H), 3.30-3.80 (m, 20H), 4.62 (t, 1H).

2-[2-(2-Hexyloxyethoxy)ethoxy]-tetrahydropyran [$CH_3(CH_2)_5(OCH_2CH_2)_2OTHP$]. Obtained as described above as a yellow oil in 95% yield. ^{1}H NMR δ 0.85 (t, 3H), 1.26 (m, 6H), 1.61-1.93 (m, 8H), 3.30-3.80 (m, 12H), 4.62 (t, 1H).

2-[2-(2-(2-(2-Hexyloxyethoxy)ethoxy)ethoxy)ethoxy]-tetrahydropyran [$CH_3(CH_2)_5(OCH_2CH_2)_4OTHP$]. Obtained as described above as a yellow oil in 90% yield. ^{1}H NMR δ 0.85 (t, 3H), 1.26 (m, 6H), 1.61-1.93 (m, 8H), 3.29-3.81 (m, 20H), 4.62 (t, 1H).

2-[2-(2-(2-(2-(2-Hexyloxyethoxy)ethoxy)ethoxy)ethoxy)ethoxy]-tetrahydropyran [$CH_3(CH_2)_5(OCH_2CH_2)_6OTHP$]. Obtained as described above as a yellow oil in 89% yield. ^{1}H NMR δ 0.85 (t, 3H), 1.26 (m, 6H), 1.61-1.93 (m, 8H), 3.30-3.80 (m, 28H), 4.62 (t, 1H).

2-[2-(2-Tetradecyloxyethoxy)ethoxy]-tetrahydropyran [$CH_3(CH_2)_{13}(OCH_2CH_2)_2OTHP$]. Obtained as described above as a yellow oil in 95% yield. ^{1}H NMR δ 0.85 (t, 3H), 1.26 (m, 22H), 1.61-1.93 (m, 8H), 3.30-3.80 (m, 12H), 4.62 (t, 1H).

2-[2-(2-(2-(2-(2-Tetradecyloxyethoxy)ethoxy)ethoxy)ethoxy)ethoxy]-tetrahydropyran [$CH_3(CH_2)_{13}(OCH_2CH_2)_6OTHP$]. Obtained as described above as a brown oil in 91% yield. ^{1}H NMR δ 0.85 (t, 3H), 1.26 (m, 22H), 1.61-1.93 (m, 8H), 3.30-3.80 (m, 28H), 4.62 (t, 1H).

2-[2-(2-(2-(2-Octyloxyethoxy)ethoxy)ethoxy)ethoxy]-tetrahydropyran [$CH_3(CH_2)_7(OCH_2CH_2)_4OTHP$]. Obtained as described above as a yellow oil in 96% yield. ^{1}H NMR δ 0.85 (t, 3H), 1.26 (m, 10H), 1.61-1.93 (m, 8H), 3.30-3.80 (m, 20H), 4.62 (t, 1H).

2-[2-(2-(2-Decyloxyethoxy)ethoxy)ethoxy]-tetrahydropyran

[$CH_3(CH_2)_9(OCH_2CH_2)_4OTHP$]. Obtained as described above as a yellow oil in 98% yield. ^{1}H NMR δ 0.85 (t, 3H), 1.26 (m, 14H), 1.61-1.93 (m, 8H), 3.30-3.80 (m, 20H), 4.62 (t, 1H).

2-[2-(2-(2-(2-Dodecyloxyethoxy)ethoxy)ethoxy)ethoxy]-tetrahydropyran

[$CH_3(CH_2)_{11}(OCH_2CH_2)_4OTHP$]. Obtained as described above as a yellow oil in 97% yield. ^{1}H NMR δ 0.85 (t, 3H), 1.26 (m, 18H), 1.61-1.93 (m, 8H), 3.30-3.80 (m, 20H), 4.62 (t, 1H).

2-[2-(2-(2-(2-Hexadecyloxyethoxy)ethoxy)ethoxy)ethoxy]-tetrahydropyran

[$CH_3(CH_2)_{15}(OCH_2CH_2)_4OTHP$]. Obtained as described above as a yellow oil in 92% yield. ^{1}H NMR δ 0.85 (t, 3H), 1.26 (m, 26H), 1.61-1.93 (m, 8H), 3.30-3.80 (m, 20H), 4.62 (t, 1H).

2-[2-(2-(2-(2-Octadecyloxyethoxy)ethoxy)ethoxy)ethoxy]-tetrahydropyran

[$CH_3(CH_2)_{17}(OCH_2CH_2)_4OTHP$]. Obtained as described above as a yellow oil in 95% yield. ^{1}H NMR δ 0.85 (t, 3H), 1.26 (m, 30H), 1.61-1.93 (m, 8H), 3.30-3.80 (m, 20H), 4.62 (t, 1H).

3,6,9,12-Tetraoxahexacosan-1-ol [$CH_3(CH_2)_{13}(OCH_2CH_2)_4OH$] ($C_{14}E_4$).

HCl (1N, 10 mL) was added to a solution of 9.5 g (20 mmol) of $CH_3(CH_2)_{13}(OCH_2CH_2)_4OTHP$ in 100 mL of ethanol. After refluxing the solution for 2h, the mixture was neutralized with sat. NaHCO$_3$ and concentrated under reduced pressure. The residue was dissolved in CHCl$_3$ (100 mL) and washed with sat. NaCl solution. The organic layer was dried over MgSO$_4$, concentrated by rotary evaporation, and dried under vacuum (20 mtorr) overnight to remove volatile impurities. The white crystalline product (7.6 g, 98%) was used in the next step without further purification. ^{1}H NMR δ 0.86 (t, 3H), 1.26 (m, 22H), 1.55 (m, 2H), 2.20 (br singlet, 1H), 3.42 (t, 2H) 3.50-3.80 (m, 16H). mp 27.0 °C (lit.[52] mp 28.5 °C).

3,6-Dioxadodecan-1-ol [$CH_3(CH_2)_5(OCH_2CH_2)_2OH$] ($C_6E_2$).

Obtained as described above as a light yellow oil in 99% yield. ^{1}H NMR δ 0.86 (t, 3H), 1.26 (m, 6H), 1.55 (m, 2H), 2.20 (br singlet, 1H), 3.42 (t, 2H) 3.50-3.80 (m, 8H). mp – 42.5 °C (lit.[53] mp – 40.2 °C).

3,6,9,12-Tetraoxaoctadecan-1-ol [$CH_3(CH_2)_5(OCH_2CH_2)_4OH$] ($C_6E_4$).

Obtained as described above as a light yellow oil in 98% yield. ^{1}H NMR δ 0.86 (t, 3H), 1.26 (m, 6H), 1.55 (m, 2H), 2.20 (br singlet, 1H), 3.42 (t, 2H) 3.50-3.80 (m, 16H). mp – 15.0 °C (lit.[54] mp –11.9 °C).

3,6,9,12,15,18-Hexaoxatetracosan-1-ol [CH$_3$(CH$_2$)$_5$(OCH$_2$CH$_2$)$_6$OH] (C$_6$E$_6$). Obtained as described above as a light yellow oil in 98% yield. ^{1}H NMR δ 0.86 (t, 3H), 1.26 (m, 6H), 1.55 (m, 2H), 2.20 (br singlet, 1H), 3.42 (t, 2H) 3.50-3.80 (m, 24H). mp – 3.5 °C (lit.[53] mp 1.2 °C).

3,6,9,12-Tetraoxaeicosan-1-ol [CH$_3$(CH$_2$)$_7$(OCH$_2$CH$_2$)$_4$OH] (C$_8$E$_4$). Obtained as described above as a light yellow oil in 98%yield. ^{1}H NMR δ 0.86 (t, 3H), 1.26 (m, 10H), 1.55 (m, 2H), 2.20 (br singlet, 1H), 3.42 (t, 2H) 3.50-3.80 (m, 16H). mp -3.2 °C (lit.[55] mp – 2.0 °C).

3,6,9,12-Tetraoxadocosan-1-ol [CH$_3$(CH$_2$)$_9$(OCH$_2$CH$_2$)$_4$OH] (C$_{10}$E$_4$). Obtained as described above as a light yellow oil in 98% yield. ^{1}H NMR δ 0.86 (t, 3H), 1.26 (m, 14H), 1.55 (m, 2H), 2.20 (br singlet, 1H), 3.42 (t, 2H) 3.50-3.80 (m, 16H). mp 8.2 °C.

3,6,9,12-Tetraoxatetracosan-1-ol [CH$_3$(CH$_2$)$_{11}$(OCH$_2$CH$_2$)$_4$OH] (C$_{12}$E$_4$). Obtained as described above as a light yellow oil in 98% yield. ^{1}H NMR δ 0.86 (t, 3H), 1.26 (m, 18H), 1.55 (m, 2H), 2.20 (br singlet, 1H), 3.42 (t, 2H) 3.50-3.80 (m, 16H). mp 18.1 °C (lit.[52] mp 20.5 °C).

3,6-Dioxaeicosan-1-ol [CH$_3$(CH$_2$)$_{13}$(OCH$_2$CH$_2$)$_2$OH] (C$_{14}$E$_2$). Obtained as described above as a white crystalline solid in 99% yield. ^{1}H NMR δ 0.86 (t, 3H), 1.26 (m, 22H), 1.55 (m, 2H), 2.20 (br singlet, 1H), 3.42 (t, 2H) 3.50-3.80 (m, 8H). mp 26.1 °C (lit.[52] mp 28.5 °C).

3,6,9,12,15,18-Hexaoxadotriacontan-1-ol [CH$_3$(CH$_2$)$_{13}$(OCH$_2$CH$_2$)$_6$OH] (C$_{14}$E$_6$). Obtained as described above as a white crystalline solid in 97% yield. ^{1}H NMR δ 0.86 (t, 3H), 1.26 (m, 22H), 1.55 (m, 2H), 2.20 (br singlet, 1H), 3.42 (t, 2H) 3.50-3.80 (m, 24H). mp 35.5 °C (lit.[56] mp 35.0 °C).

3,6,9,12-Tetraoxaoctacosan-1-ol [CH$_3$(CH$_2$)$_{15}$(OCH$_2$CH$_2$)$_4$OH] (C$_{16}$E$_4$). Obtained as described above as a white crystalline solid in 99% yield. ^{1}H NMR δ 0.86 (t, 3H), 1.26 (m, 26H), 1.55 (m, 2H), 2.20 (br singlet, 1H), 3.42 (t, 2H) 3.50-3.80 (m, 16H). mp 33.2 °C (lit.[52] mp 35.2 °C).

3,6,9,12-Tetraoxatricontan-1-ol [CH$_3$(CH$_2$)$_{17}$(OCH$_2$CH$_2$)$_4$OH] (C$_{18}$E$_4$). Obtained as described above as a white crystalline solid in 99% yield. ^{1}H NMR δ 0.86 (t, 3H), 1.26 (m, 30H), 1.55 (m, 2H), 2.20 (br singlet, 1H), 3.42 (t, 2H) 3.50-3.80 (m, 16H). mp 41.1 °C (lit.[57] mp 41.0 °C).

Synthesis of methacrylate monomers (C$_x$E$_y$MA)

3,6,9,12-Tetraoxahexacosyl methacrylate (C$_{14}$E$_4$MA). 3,6,9,12-Tetraoxahexacosanol (1.6 g, 4.0 mmol) prepared as described above and 0.81 g (8.0 mmol) of triethylamine were dissolved in 10 mL of anhydrous ether. Methacryloyl chloride (0.63 g, 6 mmol) was injected into the stirred solution over a period of 5 min. After stirring for an additional 10 min, the mixture was concentrated by rotary evaporation and then for 1 hour at 20 mtorr to remove residual triethylamine and methacryloyl chloride. The residue was dissolved in 50 mL ether, filtered, washed with 5% aqueous NaCl, dried under MgSO$_4$ and concentrated under reduced pressure. The light yellow oil was further purified by column chromatography (silica gel, 25:75 ethyl acetate/hexane) to give a clear colorless liquid (1.1 g) in 60% yield.^{1}H NMR δ 0.85 (t, 3H), 1.26 (m, 22H), 1.55 (m, 2H), 1.92 (s, 3H), 3.42 (t, 2H), 3.50-3.74 (m, 14H), 4.26 (t, 2H), 5.55 (s, 1H), 6.10 (s, 1H).

Hexyl methacrylate (C$_6$E$_0$MA). Isolated by column chromatography (silica gel, 5:95 ethyl acetate/hexane) as a clear colorless liquid (2.2 g) in 82% yield. ^{1}H NMR δ 0.85 (t, 3H), 1.26 (m, 6H), 1.62 (m, 2H), 1.92 (s, 3H), 4.11 (t, 2H) 5.55 (s, 1H), 6.10 (s, 1H).

3,6-Dioxadodecyl methacrylate (C$_6$E$_2$MA). Isolated by column chromatography (silica gel, 15:85 ethyl acetate/hexane) as a clear colorless liquid (1.5 g) in 71% yield. ^{1}H NMR δ 0.85 (t, 3H), 1.26 (m, 6H), 1.55 (m, 2H), 1.92 (s, 3H), 3.42 (t, 2H), 3.50-3.74 (m, 6H), 4.26 (t, 2H), 5.55 (s, 1H), 6.10 (s, 1H).

3,6,9,12-Tetraoxaoctadecanyl methacrylate (C$_6$E$_4$MA). Isolated by column chromatography (silica gel, 25:75 ethyl acetate/hexane) as a clear colorless liquid (1.2 g) in 63% yield. ^{1}H NMR δ 0.85 (t, 3H), 1.26 (m, 6H), 1.55 (m, 2H), 1.92 (s, 3H), 3.42 (t, 2H), 3.50-3.74 (m, 14H), 4.26 (t, 2H), 5.55 (s, 1H), 6.10 (s, 1H).

3,6,9,12,15,18-Hexaoxatetracosyl methacrylate (C$_6$E$_6$MA). Isolated by column chromatography (silica gel, 60:40 ethyl acetate/hexane) as a clear colorless liquid (0.93 g) in 55% yield. ^{1}H NMR δ 0.85 (t, 3H), 1.26 (m, 6H), 1.55 (m, 2H), 1.92 (s, 3H), 3.42 (t, 2H), 3.50-3.74 (m, 22H), 4.26 (t, 2H), 5.55 (s, 1H), 6.10 (s, 1H).

3,6,9,12-Tetraoxacosyl methacrylate (C_8E_4). Isolated by column chromatography (silica gel, 25:75 ethyl acetate/hexane) as a clear colorless liquid (1.1 g) in 45% yield. ^{1}H NMR δ 0.85 (t, 3H), 1.26 (m, 10H), 1.55 (m, 2H), 1.92 (s, 3H), 3.42 (t, 2H), 3.50-3.74 (m, 14H), 4.26 (t, 2H), 5.55 (s, 1H), 6.10 (s, 1H).

3,6,9,12-Tetraoxadocosyl methacrylate ($C_{10}E_4MA$). Isolated by column chromatography (silica gel, 25:75 ethyl acetate/hexane) as a clear colorless liquid (1.1 g) in 52% yield. Yield 1.1 g (52%). ^{1}H NMR δ 0.85 (t, 3H), 1.26 (m, 14H), 1.55 (m, 2H), 1.92 (s, 3H), 3.42 (t, 2H), 3.50-3.74 (m, 14H), 4.26 (t, 2H), 5.55 (s, 1H), 6.10 (s, 1H).

3,6,9,12-Tetraoxatetracosyl methacrylate ($C_{12}E_4MA$). Isolated by column chromatography (silica gel, 25:75 ethyl acetate/hexane) as a clear colorless liquid (1.1 g) in 68% yield. ^{1}H NMR δ 0.85 (t, 3H), 1.26 (m, 18H), 1.55 (m, 2H), 1.92 (s, 3H), 3.42 (t, 2H), 3.50-3.74 (m, 14H), 4.26 (t, 2H), 5.55 (s, 1H), 6.10 (s, 1H).

Tetradecyl methacrylate ($C_{14}E_0MA$). Isolated by column chromatography (silica gel, 5:95 ethyl acetate/hexane) as a clear colorless liquid (2.0 g) in 81% yield. ^{1}H NMR δ 0.85 (t, 3H), 1.26 (m, 22H), 1.62 (m, 2H), 1.92 (s, 3H), 4.10 (t, 2H) 5.55 (s, 1H), 6.10 (s, 1H).

3,6-Dioxaeicosyl methacrylate ($C_{14}E_2MA$). Isolated by column chromatography (silica gel, 15:85 ethyl acetate/hexane) as a clear colorless liquid (1.6 g) in 73% yield. ^{1}H NMR δ 0.85 (t, 3H), 1.26 (m, 22H), 1.55 (m, 2H), 1.92 (s, 3H), 3.42 (t, 2H), 3.50-3.74 (m, 6H), 4.26 (t, 2H), 5.55 (s, 1H), 6.10 (s, 1H).

3,6,9,12-Tetraoxaoctacosyl methacrylate ($C_{16}E_4MA$). Isolated by column chromatography (silica gel, 25:75 ethyl acetate/hexane) as a clear colorless liquid (1.2 g) in 66% yield. ^{1}H NMR δ 0.85 (t, 3H), 1.26 (m, 26H), 1.55 (m, 2H), 1.92 (s, 3H), 3.42 (t, 2H), 3.50-3.74 (m, 14H), 4.26 (t, 2H), 5.55 (s, 1H), 6.10 (s, 1H).

3,6,9,12,15,18-Hexaoxadotricontyl methacrylate($C_{14}E_6MA$). Isolated by column chromatography (silica gel, 60:40 ethyl acetate/hexane) as a clear colorless liquid (1.0 g) in 50% yield.

^{1}H NMR δ 0.85 (t, 3H), 1.26 (m, 22H), 1.55 (m, 2H), 1.92 (s, 3H), 3.42 (t, 2H), 3.50-3.74 (m, 22H), 4.26 (t, 2H), 5.55 (s, 1H), 6.10 (s, 1H).

3,6,9,12-Tetraoxatricontyl methacrylate. (C$_{18}$E$_4$MA) Isolated by column chromatography (silica gel, 25:75 ethyl acetate/hexane) as a clear colorless liquid (1.5 g) in 69% yield. ^{1}H NMR δ 0.85 (t, 3H), 1.26 (m, 30H), 1.55 (m, 2H), 1.92 (s, 3H), 3.42 (t, 2H), 3.50-3.74 (m, 14H), 4.26 (t, 2H), 5.55 (s, 1H), 6.10 (s, 1H).

Polymerizations. Solution polymerizations were set up in a dry box free of air and moisture. The monomer concentration was 1 mol/L, prepared by dissolving 1 mmol of monomer in 1 mL of a 0.001g/mL solution of AIBN in toluene. Solutions were heated and stirred at 60 °C overnight, and then the polymerizations were terminated by exposure to air, and dried under vacuum. Polymers were purified by dissolution in 10 mL of CHCl$_3$ followed by precipitation in 50 mL methanol. The polymer was collected by centrifugation, and dried under vacuum until they reached constant weight.

Polymer from hexyl methacrylate (poly(C$_6$E$_0$MA)) . A translucent gel (M_w = 116,104, PDI = 2.2). Yield 55%. ^{1}H NMR δ 0.7-1.1 (m, 6H), 1.20-1.40 (m, 6H), 1.58 (m, 2H), 1.70-2.0 (b, 2H), 3.89 (b, 2H).

Polymer from 3,6,9,12-tetraoxaoctadecanyl methacrylate (poly(C$_6$E$_4$MA)). This polymer was precipitated at –30 °C to give a translucent gel (M_w = 207,384, PDI = 1.95). Yield 33%. ^{1}H NMR δ 0.7-1.1 (m, 6H), 1.20-1.40 (m, 6H), 1.58 (m, 2H), 1.70-2.0 (b, 2H), 3.42 (t, 2H), 3.50-3.74 (m, 14H), 4.06 (b, 2H).

Polymer from 3,6,9,12,15,18-hexaoxatetracosyl methacrylate (poly(C$_6$E$_6$MA)). This polymer could not be precipitated in methanol. It was dried under vacuum to give a translucent gel (M_w = 69,777, PDI = 1.5). Yield 100%. ^{1}H NMR δ 0.7-1.1 (m, 6H), 1.20-1.40 (m, 6H), 1.58 (m, 2H), 1.70-2.0 (b, 2H), 3.42 (t, 2H), 3.50-3.74 (m, 22H), 4.06 (b, 2H).

Polymer from 3,6-dioxadodecyl methacrylate (poly(C$_8$E$_2$MA)). A translucent gel (M_w = 43,278, PDI = 2.3). Yield 41%. ^{1}H NMR δ 0.7-1.1 (m, 6H), 1.20-1.40 (m, 6H), 1.58 (m, 2H), 1.70-2.0 (b, 2H), 3.42 (t, 2H), 3.50-3.74 (m, 6H), 4.06 (b, 2H).

Polymer from 3,6,9,12-tetraoxaeicosyl methacrylate (poly(C_8E_4MA)). A translucent gel (M_w = 123,000, PDI = 2.5). Yield 95%. ^{1}H NMR δ 0.7-1.1 (m, 6H), 1.20-1.40 (m, 10H), 1.58 (m, 2H), 1.70-2.0 (b, 2H), 3.42 (t, 2H), 3.50-3.74 (m, 14H), 4.06 (b, 2H).

Polymer from 3,6,9,12-tetraoxadicosyl methacrylate (poly($C_{10}E_4MA$)). A translucent gel (M_w = 107,000, PDI = 3.0). Yield 95%. ^{1}H NMR δ 0.7-1.1 (m, 6H), 1.20-1.40 (m, 14H), 1.58 (m, 2H), 1.70-2.0 (b, 2H), 3.42 (t, 2H), 3.50-3.74 (m, 14H), 4.06 (b, 2H).

Polymer from 3,6,9,12-tetraoxatetracosyl methacrylate (poly($C_{12}E_4MA$)). A translucent gel (M_w = 306,000, PDI = 2.0). Yield 95%. ^{1}H NMR δ 0.7-1.1 (m, 6H), 1.20-1.40 (m, 18H), 1.58 (m, 2H), 1.70-2.0 (b, 2H), 3.42 (t, 2H), 3.50-3.74 (m, 14H), 4.06 (b, 2H).

Polymer from tetradecyl methacrylate (poly($C_{14}E_0MA$)). A translucent gel (M_w = 100,286, PDI = 2.5). Yield 92%. ^{1}H NMR δ 0.7-1.1 (m, 6H), 1.20-1.40 (m, 22H), 1.58 (m, 2H), 1.70-2.0 (b, 2H), 3.89 (b, 2H).

Polymer from 3,6-dioxaeicosyl methacrylate (poly($C_{14}E_2MA$)). A translucent gel (M_w = 152,953, PDI = 2.9). Yield 88%. ^{1}H NMR δ 0.7-1.1 (m, 6H), 1.20-1.40 (m, 22H), 1.58 (m, 2H), 1.70-2.0 (b, 2H), 3.42 (t, 2H), 3.50-3.74 (m, 6H), 4.06 (b, 2H).

Polymer from 3,6,9,12-tetraoxahexacosyl methacrylate (poly($C_{14}E_4MA$)). A translucent gel (M_w = 171,148, PDI = 3.1). Yield 95%. ^{1}H NMR δ 0.7-1.1 (m, 6H), 1.20-1.40 (m, 22H), 1.58 (m, 2H), 1.70-2.0 (b, 2H), 3.42 (t, 2H), 3.50-3.74 (m, 14H), 4.06 (b, 2H).

Polymer from 3,6,9,12,15,18-hexaoxadotricontyl methacrylate (poly($C_{14}E_6MA$)). A translucent gel (M_w = 68,976, PDI = 1.6). Yield 90%. ^{1}H NMR δ 0.7-1.1 (m, 6H), 1.20-1.40 (m, 22H), 1.58 (m, 2H), 1.70-2.0 (b, 2H), 3.42 (t, 2H), 3.50-3.74 (m, 22H), 4.06 (b, 2H).

Polymer from 3,6,9,12-tetraoxaoctacosyl methacrylate (poly($C_{16}E_4MA$)). A white crystalline powder (M_w = 172,932, PDI = 3.3). Yield 92%. ^{1}H NMR δ 0.7-1.1 (m, 6H), 1.20-1.40 (m, 26H), 1.58 (m, 2H), 1.70-2.0 (b, 2H), 3.42 (t, 2H), 3.50-3.74 (m, 14H), 4.06 (b, 2H).

Polymer from 3,6,9,12-tetraoxatricontyl methacrylate (poly($C_{18}E_4MA$)). A white crystalline powder (M_w = 182,601, PDI = 2.9). Yield 94%. ^{1}H NMR δ 0.7-1.1 (m, 6H), 1.20-1.40 (m, 30H), 1.58 (m, 2H), 1.70-2.0 (b, 2H), 3.42 (t, 2H), 3.50-3.74 (m, 14H), 4.06 (b, 2H).

REFERENCES

1. Javaid, A., *Chem. Eng. J.* **2005,** 112, 219.

2. Pandey, P.; Chauhan, R. S., *Prog. Polym. Sci.* **2001,** 26, 853.

3. Koros, W. J.; Fleming, G. K., *J. Membr. Sci.* **1993,** 83, 1.

4. Smitha, B.; Sridhar, S.; Khan, A. A., *J. Membr. Sci.* **2005,** 259, 10.

5. Souzy, R.; Ameduri, B., *Prog. Polym. Sci.* **2005,** 30, 644.

6. Li, Q. F.; He, R. H.; Jensen, J. O.; Bjerrum, N. J., *Chem. Mat.* **2003,** 15, 4896.

7. Rikukawa, M.; Sanui, K., *Prog. Polym. Sci.* **2000,** 25, 1463.

8. Hickner, M. A.; Ghassemi, H.; Kim, Y. S.; Einsla, B. R.; McGrath, J. E., **2004,** 104, 4587-4611.

9. Xu, K., *Chem. Rev.* **2004,** 104, 4303-4417.

10. Meyer, W. H., *Adv. Mater.* **1998,** 10, 439-448.

11. Bruce, P. G.; Vincent, C. A., *J. Chem. Soc. Faraday Trans.* **1993,** 89, 3187-3203.

12. Liu, G.; Reinhout, M. T.; Baker, G. L., **2004,** 175, 721-724.

13. Mansky, P.; DeRouchey, J.; Russell, T. P.; Mays, J.; Pitsikalis, M.; Morkved, T.; Jaeger, H., *Macromolecules* **1998,** 31, 4399-4401.

14. Appetecchi, G. B.; Romagnoli, P.; Scrosati, B., *Electrochem Commun* **2001,** V3, 281-284.

15. Trapa, P. E.; Huang, B.; Won, Y.-Y.; Sadoway, D. R.; Mayes, A. M., **2002,** 5, A85-A88.

16. Trapa, P. E.; Won, Y. Y.; Mui, S. C.; Olivetti, E. A.; Huang, B. Y.; Sadoway, D. R.; Mayes, A. M.; Dallek, S., **2005,** 152, A1-A5.

17. Florjanczyk, Z.; Marcinek, M.; Wieczorek, W.; Langwald, N., *Pol. J. Chem.* **2004,** 78, 1279-1304.

18. Khan, S. A.; Baker, G. L.; Colson, S., *Chem Mater* **1994,** V6, 2359-2363.

19. Wieczorek, W.; Florjanczyk, Z.; Stevens, J. R., *Electrochim Acta* **1995,** V40, 2251-2258.

20. Walls, H. J.; Zhou, J.; Yerian, J. A.; Fedkiw, P. S.; Khan, S. A.; Stowe, M. K.; Baker, G. L., *J Power Sources* **2000,** V89, 156-162.

21. Zheng, Y. G.; Wan, G. X., *J. Appl. Polym. Sci.* **1995,** 57, 623-629.

22. Chung, J. S.; Sohn, H. J., *J. Power Sources* **2002,** 112, 671-675.

23. Albinsson, I.; Jacobsson, P.; Mellander, B. E.; Stevens, J. R., *Solid State Ionics* **1992,** 53-6, 1044-1053.

24. Cho, K. Y.; Lee, K. H.; Park, J. K., *Polym. J.* **2000,** 32, 537-542.

25. Sun, X. G.; Kerr, J. B.; Reeder, C. L.; Liu, G.; Han, Y. B., *Macromolecules* **2004,** 37, 5133-5135.

26. Sun, X. G.; Reeder, C. L.; Kerr, J. B., *Macromolecules* **2004,** 37, 2219-2227.

27. Matsumi, N.; Mizumo, T.; Ohno, H., *Chem. Lett.* **2004,** 33, 372-373.

28. Zhao, F.; Wang, M. K.; Qi, L.; Dong, S. J., *J. Solid State Electrochem.* **2004,** 8, 283-289.

29.   Kang, Y. S.; Sohn, B. H.; Jung, J. C.; Zin, W. C., *Macromol. Chem. Phys.* **2001,** 202, 2992-2998.

30.   Ikeda, Y.; Masui, H.; Syoji, S.; Sakashita, T.; Matoba, Y.; Kohjiya, S., *Polym. Int.* **1997,** 43, 269-273.

31.   Ikeda, Y.; Wada, Y.; Matoba, Y.; Murakami, S.; Kohjiya, S., *Electrochim. Acta* **2000,** 45, 1167-1174.

32.   Fish, D.; Khan, I. M.; Wu, E.; Smid, J., *Brit. Polym. J.* **1988,** 20, 281-288.

33.   Wang, L. M.; Weber, W. P., *Macromolecules* **1993,** 26, 969-974.

34.   Snyder, J. F.; Ratner, M. A.; Shriver, D. F., *J. Electrochem. Soc.* **2003,** 150, A1090-A1094.

35.   Han, S.; Hagiwara, M.; Ishizone, T., *Macromolecules* **2003,** 36, 8312.

36.   Asfour, F.; Ruud, C. J.; Baker, G. L., *submitted to J. Polym. Sci., Polym. Chem.*

37.   Plate, N. A.; Shibaev, V. P., *J. Polym. Sci., Part D, Macromol. Rev.* **1974,** 8, 117-253.

38.   Jordan, E. F.; Feldeise, D. W.; Wrigley, A. N., *J. Polym. Sci. Part A-1, Polym. Chem.* **1971,** 9, 1835.

39.   Greenberg, S. A.; Alfrey, T., *J. Am. Chem. Soc.* **1954,** 76, 6280.

40.   Mogri, Z.; Paul, D. R., *Polymer* **2001,** 42, 7765-7780.

41.   O'Leary, K.; Paul, D. R., *Polymer* **2004,** 45, 6575.

42.   Shibasaki, Y.; Fukuda, K., *J. Polym. Sci. Part A, Polym. Chem.* **1980,** 18, 2437.

43.   Borisova, T. I.; Burshtein, L. I.; Nikonorova, N. A.; Shibaev, V. P.; Moiseenko, V. M.; Plate, N. A., *Vysokomol. Soedin. A* **1977,** 19, 1218.

44.   Magagnini, P. L.; Andruzzi, F.; Benetti, G. F., *Macromolecules* **1980,** 13, 12-15.

45.   Jones, A. T., *Makromol. Chem.* **1964,** 71, 1.

46.   Kricheldorf, H. R.; Domschke, A., *Macromolecules* **1996,** 29, 1337.

47.   Kricheldorf, H. R.; Domschke, A., *Macromolecules* **1994,** 27, 1509.

48.   Hsu, W. P.; Levon, K.; Ho, K. S.; Myerson, A. S.; Kwei, T. K., *Macromolecules* **1993,** 26, 1318.

49.   Hsieh, H. W. S.; Post, B.; Morawetz, H., *J. Polym. Sci. Part B-Polym. Phys.* **1976,** 14, 1241.

50.   Chen, Y. Y.; Baker, G. L., *J. Org. Chem.* **1999,** 64, 6870.

51.   Chen, Y. Y.; Baker, G. L.; Ding, Y. Q.; Rabolt, J. F., *J. Am. Chem. Soc.* **1999,** 121, 6962.

52.   Wrigley, A. N., *J. Org. Chem.* **1960,** 25, 439-444.

53.   Mulley, B. A., *J. Chem. Soc.* **1958**, 2065-2066.

54.   Kucharski, S.; Sokolows, A.; Burczyk, B., *Rocz. Chem.* **1973,** 47.

55.   Chakhovskoy, N.; Martin, R. H.; van Nechel, R., *Bull. Soc. Chim. Belg.* **1956,** 65, 453-473.

56.   Gingras, B. A.; Bayley, C. H., *Can. J. Chem.* **1957,** 35, 599-604.

57.   Echegoyen, L. E., *J. Am. Chem. Soc.* **1989,** 111, 2440-2443.